P9.3 THE WINTER STORM LOTHAR: AN INTEGRATED VIEW ON DOPPLER RADARS, GROUND WINDS AND FOREST DAMAGE IN NORTHERN SWITZERLAND

Willi Schmid* and Marc Wüest,
Atmospheric Science, ETH, CH-8093 Zürich, Switzerland

Matthias Dobbertin
Swiss Federal Institute WSL, CH-8903 Birmensdorf, Switzerland

Jean-Philippe Schütz
Forest Sciences, FOWI-ETH, CH-8092 Zürich, Switzerland

1. INTRODUCTION

The winter storm Lothar from 26 December 1999 devastated many regions in northern France, southern Germany and northern Switzerland. People were killed in all three countries, and the wind damage, especially in the forests, was enormeous. About 12 Mio m^3 wood was broken or uprooted in the Swiss forests (WSL and BUWAL, 2001). The storm originated as a shallow low-level cyclone over the western Atlantic. The dynamical aspects of the storm on a synoptic scale are investigated by Wernli et al. (2001). The evolution of meteorological fields on the mesoscale over northern Switzerland was successfully simulated with the high-resolution MC2-model (Maurer, 2000). That simulation, however, failed to replicate the narrow cold-frontal rainband (NCFR) associated with the most severe winds and its internal dynamical structure.

The main purpose of this contribution therefore is to document the evolution of the storm seen with Doppler radar. Data of storm damage is matched with the radar data. As a result, we will show that irregularities in the damage patterns can be associated to the specific internal structure of the NCFR. We will first summarize the damage observations. Then, the radar fields are shown and associated to the damage data. We will end with a summary of the results and with concluding remarks.

2. DAMAGE SURVEY

Information on uprooted and broken trees are obtained from aerial photographs (collected and analysed by the "Bundesamt für Umwelt, Wald und Landschaft" BUWAL and FOWI-ETH) and ground surveys (undertaken by WSL, FOWI-ETH and others).

Of special interest are 2 quantities: the severity of damage in a given area and the fall direction of the broken or uprooted trees. The latter quantity is a footprint of the main direction of the wind gusts. The aerial photographs are a good base to evaluate both quantities over wide areas. Fig. 1 shows the estimated severity of damage to forests in Central and Northern Switzerland. It can be seen that W-E oriented tracks of severe damage exist. Gaps in these tracks are due to highly urbanized areas with few or no forests at all.

In contrast to damage, the analysis of the fall direction of the trees is still in progress. We show, as an example, a close-up from an aerial photograph (Fig. 2). The location of the close-up, near Bremgarten, is indicated in Fig. 4. The close-up shows fall directions mainly from W to E. However, some spatial variability is evident in this example. In the southwestern corner of the image, the fall direction is biased towards NW-SE direction, possibly caused by diverging airflow.

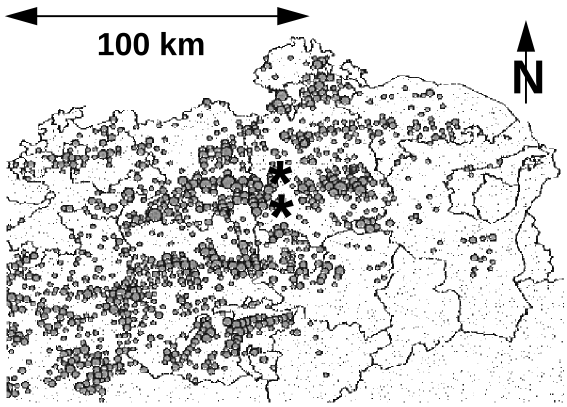

Fig. 1: Forest damage by Lothar in northern Switzerland. By courtesy of "Scherrer Ingenieurbüro AG, Nesslau". Two stars mark the locations of the ETH-radar (north) and the Albis radar (south).

* *Corresponding author address*: Willi Schmid, Atmospheric Science, ETH, CH-8093 Zurich, Switzerland, e-mail: schmid@atmos.umnw.ethz.ch

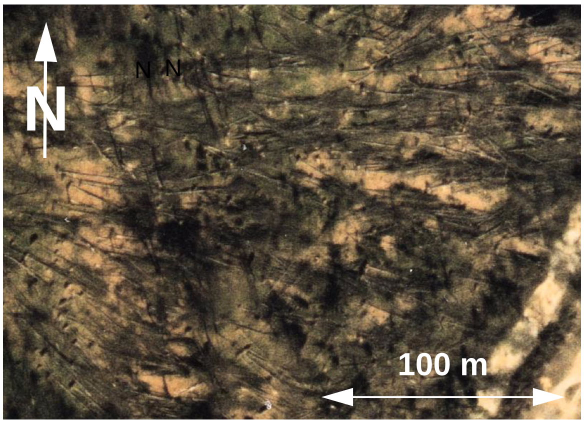

Fig. 2: Close-up from an aerial photograph, showing broken and uprooted trees near Bremgarten. The location of the close-up is given in Fig. 4.

3. RADAR SURVEY

Data from two Doppler weather radars are of interest for this study. The first is a C-band Doppler radar located in Zurich and operated by ETH (Li et al. 1995). PPI-scans at 1.5 and 20^{o} elevation angles are available every 5 min. The second radar is a C-band Doppler radar operated by MeteoSwiss (Joss et al. 1998). This radar is located on the Albis-mountain, about 14 km south of the ETH-radar. Volume scans (20 revolutions) are made every 5 min with this radar. The locations of the two radars are indicated in Fig. 1.

Fig. 3 shows a PPI of reflectivity and Doppler velocity, obtained on 26 Dec 1999, 1044 UTC, with the ETH-radar. The reflectivity PPI shows a banded structure with core regions and gap regions, often observed in “narrow cold frontal rainbands” (NCFR) and attributed to shearing instability (e.g., Hobbs and Persson 1982). A similar structure is also visible in the Doppler velocity pattern (Fig. 3b). Bands of (relatively) weak Doppler velocity can be attributed to the core regions of reflectivity. These Doppler bands are slightly shifted towards the south when compared to the core regions. Zooming into the western core region (at position 660 km east/240 km north), one notes extreme Doppler velocities (up to 60 m/s) just north of the core region.

These structures disagree with earlier observations and conceptual models of NCFR’s, indicating the strongest winds ahead of the frontal convergence line (e.g., Fig. 13 in Wakimoto and Bosart 2000). Here, the strongest winds occurred behind the convergence line. This discrepancy calls for a more detailed analysis of the rainbands. The favorable position of the rainband around 1044 UTC makes it possible to perform a dual-Doppler wind analysis.

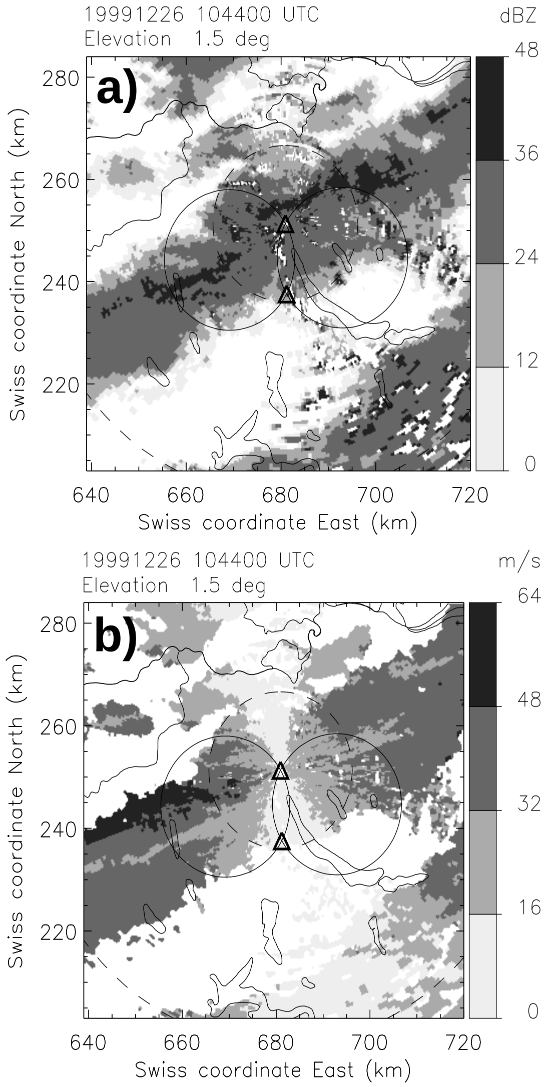

Fig. 3: PPI of reflectivity (a) and Doppler velocity (b), as observed with the ETH-radar on 26 Dec 1999, 1044 UTC. Note that the absolute value of Doppler velocity is shown in (b).

The dealiasing of the ETH-Doppler data was done with a variational procedure (Wüest et al. 2000). The Doppler data from the Albis radar were dealiased by eye, since the extreme winds, substantial shear zones and a low Nyquist velocity (8 m/s, compared to 16 m/s for the ETH-radar) make an automated unfolding difficult. The dual-Doppler analysis was done with the procedure by Protat and Zawadzki (1999), adapted for Swiss conditions by Wüest et al. (2001). The PPIs were interpolated onto a common time considering the mean motion of the rainband. Fig. 4 shows the result for a part of the dual-Doppler region in the west of the two radars. Fig. 4a shows the ground-relative winds, and Fig. 4b shows the storm-relative winds.

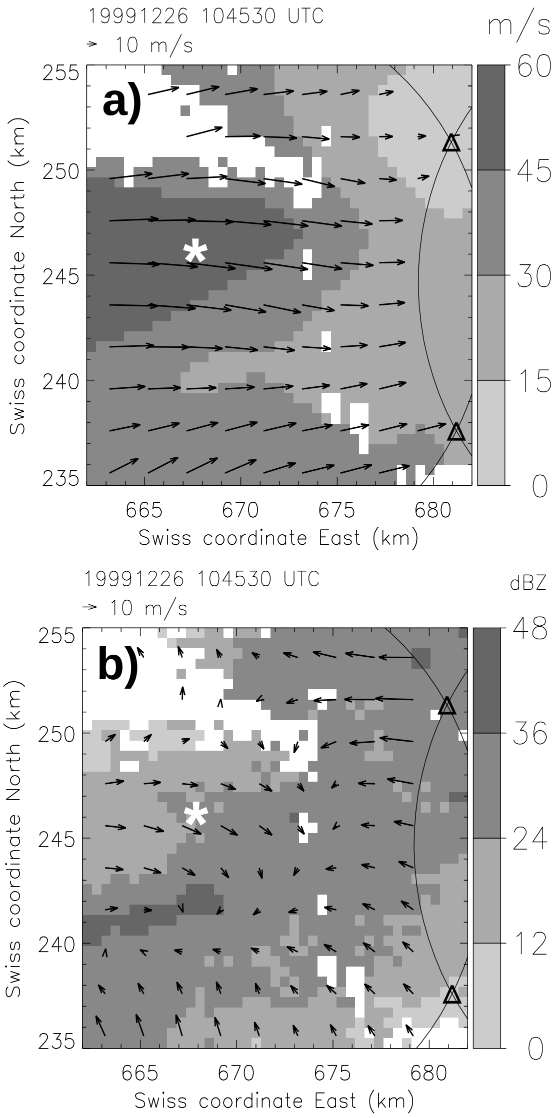

Fig. 4: (a) Ground-relative dual-Doppler wind vectors (radars ETH/Albis) and wind speed (grey-shaded), and (b) Storm-relative dual-Doppler wind vectors and radar reflectivity (grey-shaded). The location of the damage shown in Fig. 2 is indicated with a star in (a) and (b).

The figure indicates two important features: first, substantial convergence south of the core region in the SW-part of the domain, second, a downburst-like outflow region north of the core region. The heaviest wind gusts occurred in that outflow region. The wind direction is from W to WNW, which is in a good agreement with the fall direction of the broken trees, see Fig. 2.

4. CONCLUSIONS

In this study we compared severe forest damage due to the storm Lothar with Doppler data from two radars (ETH and Albis) in northern Switzerland. A banded structure can be seen in the damage patterns. Based on the analysis of the radar data, we can explain the banded structure as follows: the strongest winds were associated with a "narrow cold-frontal rainband" (NCFR), further subdivided in so-called core regions and gap regions. The core regions were accompanied by a marked convergence line (south of the reflectivity cores) and downburst-like stripes of severe winds (north of the reflectivity cores). It is suggested that several similar stripes of heavy wind were responsible for the banded structure of the forest damage.

ACKNOWLEDGEMENTS

We would like to thank MeteoSwiss for the Albis radar data. The map of Lothar damage (Fig. 1), kindly provided by "Scherrer Ingenieurbüro AG, Nesslau", was established within the project "BUWAL/L+T Gesamtschweizerische Erfassung der Sturmschäden Lothar".

REFERENCES

Hobbs, P.V. and P.O. Persson, 1982: The mesoscale and microscale structure and organization of clouds and precipitation in midlatitude cyclones. Part V: The substructure of narrow cold-frontal rainbands. *J. Atmos. Sci.*, **39**, 280-295.

Joss, J., et al., 1998: Operational use of radar for precipitation measurements in Switzerland. Final Report NRP 31. VDF Hochschulverlag AG an der ETH Zürich, 108 pp.

Li, L., W. Schmid and J. Joss, 1995: Nowcasting of motion and growth of precipitation with radar over a complex orography. *J. Appl. Meteor.*, **31**, 1286-1300.

Maurer, T., 2000: Untersuchung der Sturmwinde von Lothar mit dem hochauflösenden Wettervorhersagemodell MC2. Diploma Work, Institut für Klimaforschung, ETHZ, 87 pp.

Protat, A., and I. Zawadzki, 1999: A variational method for real-time retrieval of three-dimensional wind field from multiple-Doppler bistatic radar network data. *J. Atmos. Oceanic. Tech.*, **16**, 432-449.

Wakimoto, R.M. and B.L. Bosart, 2000: Airborne radar observations of a cold front during FASTEX. *Mon. Wea. Rev.*, **128**, 2447-2470.

Wernli, H., S. Dirren, M. Liniger, and M. Zillig, 2001: Dynamical aspects of the life cycle of the winter storm 'Lothar' (24-26 December 1999). Submitted to *Q. J. R. Meteorol. Soc*.

WSL and BUWAL, 2001: Lothar. Der Orkan 1999. Ereignisanalyse. Birmensdorf und Bern, Eidg. Forschungsanstalt WSL und Bundesamt für Umwelt, Wald und Landschaft, 400 pp.

Wüest, M, U. Germann and W. Schmid, 2000: A variational de-aliasing technique. *Phys. Chem. Earth (B)*, **25**, 1179-1183.

Wüest, M., I. Zawadzki and W. Schmid, 2001: Noise filtering in a variational wind field retrieval from Doppler radar. Meteorol. Z., in press.